FERMILAB-PUB-06-345-E

Measurement of the W boson helicity in top quark decay at DØ

V.M. Abazov,[35] B. Abbott,[75] M. Abolins,[65] B.S. Acharya,[28] M. Adams,[51] T. Adams,[49] M. Agelou,[17] E. Aguilo,[5] S.H. Ahn,[30] M. Ahsan,[59] G.D. Alexeev,[35] G. Alkhazov,[39] A. Alton,[64] G. Alverson,[63] G.A. Alves,[2] M. Anastasoaie,[34] T. Andeen,[53] S. Anderson,[45] B. Andrieu,[16] M.S. Anzelc,[53] Y. Arnoud,[13] M. Arov,[52] A. Askew,[49] B. Åsman,[40] A.C.S. Assis Jesus,[3] O. Atramentov,[49] C. Autermann,[20] C. Avila,[7] C. Ay,[23] F. Badaud,[12] A. Baden,[61] L. Bagby,[52] B. Baldin,[50] D.V. Bandurin,[59] P. Banerjee,[28] S. Banerjee,[28] E. Barberis,[63] P. Bargassa,[80] P. Baringer,[58] C. Barnes,[43] J. Barreto,[2] J.F. Bartlett,[50] U. Bassler,[16] D. Bauer,[43] S. Beale,[5] A. Bean,[58] M. Begalli,[3] M. Begel,[71] C. Belanger-Champagne,[5] L. Bellantoni,[50] A. Bellavance,[67] J.A. Benitez,[65] S.B. Beri,[26] G. Bernardi,[16] R. Bernhard,[41] L. Berntzon,[14] I. Bertram,[42] M. Besançon,[17] R. Beuselinck,[43] V.A. Bezzubov,[38] P.C. Bhat,[50] V. Bhatnagar,[26] M. Binder,[24] C. Biscarat,[42] K.M. Black,[62] I. Blackler,[43] G. Blazey,[52] F. Blekman,[43] S. Blessing,[49] D. Bloch,[18] K. Bloom,[67] U. Blumenschein,[22] A. Boehnlein,[50] O. Boeriu,[55] T.A. Bolton,[59] G. Borissov,[42] K. Bos,[33] T. Bose,[77] A. Brandt,[78] R. Brock,[65] G. Brooijmans,[70] A. Bross,[50] D. Brown,[78] N.J. Buchanan,[49] D. Buchholz,[53] M. Buehler,[81] V. Buescher,[22] S. Burdin,[50] S. Burke,[45] T.H. Burnett,[82] E. Busato,[16] C.P. Buszello,[43] J.M. Butler,[62] P. Calfayan,[24] S. Calvet,[14] J. Cammin,[71] S. Caron,[33] W. Carvalho,[3] B.C.K. Casey,[77] N.M. Cason,[55] H. Castilla-Valdez,[32] S. Chakrabarti,[28] D. Chakraborty,[52] K.M. Chan,[71] A. Chandra,[48] F. Charles,[18] E. Cheu,[45] F. Chevallier,[13] D.K. Cho,[62] S. Choi,[31] B. Choudhary,[27] L. Christofek,[77] D. Claes,[67] B. Clément,[18] C. Clément,[40] Y. Coadou,[5] M. Cooke,[80] W.E. Cooper,[50] D. Coppage,[58] M. Corcoran,[80] M.-C. Cousinou,[14] B. Cox,[44] S. Crépé-Renaudin,[13] D. Cutts,[77] M. Ćwiok,[29] H. da Motta,[2] A. Das,[62] M. Das,[60] B. Davies,[42] G. Davies,[43] G.A. Davis,[53] K. De,[78] P. de Jong,[33] S.J. de Jong,[34] E. De La Cruz-Burelo,[64] C. De Oliveira Martins,[3] J.D. Degenhardt,[64] F. Déliot,[17] M. Demarteau,[50] R. Demina,[71] P. Demine,[17] D. Denisov,[50] S.P. Denisov,[38] S. Desai,[72] H.T. Diehl,[50] M. Diesburg,[50] M. Doidge,[42] A. Dominguez,[67] H. Dong,[72] L.V. Dudko,[37] L. Duflot,[15] S.R. Dugad,[28] D. Duggan,[49] A. Duperrin,[14] J. Dyer,[65] A. Dyshkant,[52] M. Eads,[67] D. Edmunds,[65] T. Edwards,[44] J. Ellison,[48] J. Elmsheuser,[24] V.D. Elvira,[50] S. Eno,[61] P. Ermolov,[37] H. Evans,[54] A. Evdokimov,[36] V.N. Evdokimov,[38] S.N. Fatakia,[62] L. Feligioni,[62] A.V. Ferapontov,[59] T. Ferbel,[71] F. Fiedler,[24] F. Filthaut,[34] W. Fisher,[50] H.E. Fisk,[50] I. Fleck,[22] M. Ford,[44] M. Fortner,[52] H. Fox,[22] S. Fu,[50] S. Fuess,[50] T. Gadfort,[82] C.F. Galea,[34] E. Gallas,[50] E. Galyaev,[55] C. Garcia,[71] A. Garcia-Bellido,[82] J. Gardner,[58] V. Gavrilov,[36] A. Gay,[18] P. Gay,[12] D. Gelé,[18] R. Gelhaus,[48] C.E. Gerber,[51] Y. Gershtein,[49] D. Gillberg,[5] G. Ginther,[71] B. Gmyrek,[45] N. Gollub,[40] B. Gómez,[7] A. Goussiou,[55] P.D. Grannis,[72] H. Greenlee,[50] Z.D. Greenwood,[60] E.M. Gregores,[4] G. Grenier,[19] Ph. Gris,[12] J.-F. Grivaz,[15] S. Grünendahl,[50] M.W. Grünewald,[29] F. Guo,[72] J. Guo,[72] G. Gutierrez,[50] P. Gutierrez,[75] A. Haas,[70] N.J. Hadley,[61] P. Haefner,[24] S. Hagopian,[49] J. Haley,[68] I. Hall,[75] R.E. Hall,[47] L. Han,[6] K. Hanagaki,[50] P. Hansson,[40] K. Harder,[59] A. Harel,[71] R. Harrington,[63] J.M. Hauptman,[57] R. Hauser,[65] J. Hays,[53] T. Hebbeker,[20] D. Hedin,[52] J.G. Hegeman,[33] J.M. Heinmiller,[51] A.P. Heinson,[48] U. Heintz,[62] C. Hensel,[58] K. Herner,[72] G. Hesketh,[63] M.D. Hildreth,[55] R. Hirosky,[81] J.D. Hobbs,[72] B. Hoeneisen,[11] H. Hoeth,[25] M. Hohlfeld,[15] S.J. Hong,[30] R. Hooper,[77] P. Houben,[33] Y. Hu,[72] Z. Hubacek,[9] V. Hynek,[8] I. Iashvili,[69] R. Illingworth,[50] A.S. Ito,[50] S. Jabeen,[62] M. Jaffré,[15] S. Jain,[75] K. Jakobs,[22] C. Jarvis,[61] A. Jenkins,[43] R. Jesik,[43] K. Johns,[45] C. Johnson,[70] M. Johnson,[50] A. Jonckheere,[50] P. Jonsson,[43] A. Juste,[50] D. Käfer,[20] S. Kahn,[73] E. Kajfasz,[14] A.M. Kalinin,[35] J.M. Kalk,[60] J.R. Kalk,[65] S. Kappler,[20] D. Karmanov,[37] J. Kasper,[62] P. Kasper,[50] I. Katsanos,[70] D. Kau,[49] R. Kaur,[26] R. Kehoe,[79] S. Kermiche,[14] N. Khalatyan,[62] A. Khanov,[76] A. Kharchilava,[69] Y.M. Kharzheev,[35] D. Khatidze,[70] H. Kim,[78] T.J. Kim,[30] M.H. Kirby,[34] B. Klima,[50] J.M. Kohli,[26] J.-P. Konrath,[22] M. Kopal,[75] V.M. Korablev,[38] J. Kotcher,[73] B. Kothari,[70] A. Koubarovsky,[37] A.V. Kozelov,[38] D. Krop,[54] A. Kryemadhi,[81] T. Kuhl,[23] A. Kumar,[69] S. Kunori,[61] A. Kupco,[10] T. Kurča,[19,*] J. Kvita,[8] S. Lammers,[70] G. Landsberg,[77] J. Lazoflores,[49] A.-C. Le Bihan,[18] P. Lebrun,[19] W.M. Lee,[52] A. Leflat,[37] F. Lehner,[41] V. Lesne,[12] J. Leveque,[45] P. Lewis,[43] J. Li,[78] Q.Z. Li,[50] J.G.R. Lima,[52] D. Lincoln,[50] J. Linnemann,[65] V.V. Lipaev,[38] R. Lipton,[50] Z. Liu,[5] L. Lobo,[43] A. Lobodenko,[39] M. Lokajicek,[10] A. Lounis,[18] P. Love,[42] H.J. Lubatti,[82] M. Lynker,[55] A.L. Lyon,[50] A.K.A. Maciel,[2] R.J. Madaras,[46] P. Mättig,[25] C. Magass,[20] A. Magerkurth,[64] A.-M. Magnan,[13] N. Makovec,[15] P.K. Mal,[55] H.B. Malbouisson,[3] S. Malik,[67] V.L. Malyshev,[35] H.S. Mao,[50] Y. Maravin,[59] M. Martens,[50] R. McCarthy,[72] D. Meder,[23] A. Melnitchouk,[66] A. Mendes,[14] L. Mendoza,[7] M. Merkin,[37] K.W. Merritt,[50] A. Meyer,[20] J. Meyer,[21] M. Michaut,[17] H. Miettinen,[80] T. Millet,[19] J. Mitrevski,[70] J. Molina,[3] N.K. Mondal,[28] J. Monk,[44] R.W. Moore,[5] T. Moulik,[58] G.S. Muanza,[15] M. Mulders,[50] M. Mulhearn,[70] O. Mundal,[22] L. Mundim,[3] Y.D. Mutaf,[72]

E. Nagy,[14] M. Naimuddin,[27] M. Narain,[62] N.A. Naumann,[34] H.A. Neal,[64] J.P. Negret,[7] P. Neustroev,[39] C. Noeding,[22] A. Nomerotski,[50] S.F. Novaes,[4] T. Nunnemann,[24] V. O'Dell,[50] D.C. O'Neil,[5] G. Obrant,[39] V. Oguri,[3] N. Oliveira,[3] D. Onoprienko,[59] N. Oshima,[50] R. Otec,[9] G.J. Otero y Garzón,[51] M. Owen,[44] P. Padley,[80] N. Parashar,[56] S.-J. Park,[71] S.K. Park,[30] J. Parsons,[70] R. Partridge,[77] N. Parua,[72] A. Patwa,[73] G. Pawloski,[80] P.M. Perea,[48] E. Perez,[17] K. Peters,[44] P. Pétroff,[15] M. Petteni,[43] R. Piegaia,[1] J. Piper,[65] M.-A. Pleier,[21] P.L.M. Podesta-Lerma,[32] V.M. Podstavkov,[50] Y. Pogorelov,[55] M.-E. Pol,[2] A. Pompoš,[75] B.G. Pope,[65] A.V. Popov,[38] C. Potter,[5] W.L. Prado da Silva,[3] H.B. Prosper,[49] S. Protopopescu,[73] J. Qian,[64] A. Quadt,[21] B. Quinn,[66] M.S. Rangel,[2] K.J. Rani,[28] K. Ranjan,[27] P.N. Ratoff,[42] P. Renkel,[79] S. Reucroft,[63] M. Rijssenbeek,[72] I. Ripp-Baudot,[18] F. Rizatdinova,[76] S. Robinson,[43] R.F. Rodrigues,[3] C. Royon,[17] P. Rubinov,[50] R. Ruchti,[55] V.I. Rud,[37] G. Sajot,[13] A. Sánchez-Hernández,[32] M.P. Sanders,[61] A. Santoro,[3] G. Savage,[50] L. Sawyer,[60] T. Scanlon,[43] D. Schaile,[24] R.D. Schamberger,[72] Y. Scheglov,[39] H. Schellman,[53] P. Schieferdecker,[24] C. Schmitt,[25] C. Schwanenberger,[44] A. Schwartzman,[68] R. Schwienhorst,[65] J. Sekaric,[49] S. Sengupta,[49] H. Severini,[75] E. Shabalina,[51] M. Shamim,[59] V. Shary,[17] A.A. Shchukin,[38] W.D. Shephard,[55] R.K. Shivpuri,[27] D. Shpakov,[50] V. Siccardi,[18] R.A. Sidwell,[59] V. Simak,[9] V. Sirotenko,[50] P. Skubic,[75] P. Slattery,[71] R.P. Smith,[50] G.R. Snow,[67] J. Snow,[74] S. Snyder,[73] S. Söldner-Rembold,[44] X. Song,[52] L. Sonnenschein,[16] A. Sopczak,[42] M. Sosebee,[78] K. Soustruznik,[8] M. Souza,[2] B. Spurlock,[78] J. Stark,[13] J. Steele,[60] V. Stolin,[36] A. Stone,[51] D.A. Stoyanova,[38] J. Strandberg,[64] S. Strandberg,[40] M.A. Strang,[69] M. Strauss,[75] R. Ströhmer,[24] D. Strom,[53] M. Strovink,[46] L. Stutte,[50] S. Sumowidagdo,[49] P. Svoisky,[55] A. Sznajder,[3] M. Talby,[14] P. Tamburello,[45] W. Taylor,[5] P. Telford,[44] J. Temple,[45] B. Tiller,[24] M. Titov,[22] V.V. Tokmenin,[35] M. Tomoto,[50] T. Toole,[61] I. Torchiani,[22] S. Towers,[42] T. Trefzger,[23] S. Trincaz-Duvoid,[16] D. Tsybychev,[72] B. Tuchming,[17] C. Tully,[68] A.S. Turcot,[44] P.M. Tuts,[70] R. Unalan,[65] L. Uvarov,[39] S. Uvarov,[39] S. Uzunyan,[52] B. Vachon,[5] P.J. van den Berg,[33] R. Van Kooten,[54] W.M. van Leeuwen,[33] N. Varelas,[51] E.W. Varnes,[45] A. Vartapetian,[78] I.A. Vasilyev,[38] M. Vaupel,[25] P. Verdier,[19] L.S. Vertogradov,[35] M. Verzocchi,[50] F. Villeneuve-Seguier,[43] P. Vint,[43] J.-R. Vlimant,[16] E. Von Toerne,[59] M. Voutilainen,[67,†] M. Vreeswijk,[33] H.D. Wahl,[49] L. Wang,[61] M.H.L.S Wang,[50] J. Warchol,[55] G. Watts,[82] M. Wayne,[55] G. Weber,[23] M. Weber,[50] H. Weerts,[65] N. Wermes,[21] M. Wetstein,[61] A. White,[78] D. Wicke,[25] G.W. Wilson,[58] S.J. Wimpenny,[48] M. Wobisch,[50] J. Womersley,[50] D.R. Wood,[63] T.R. Wyatt,[44] Y. Xie,[77] N. Xuan,[55] S. Yacoob,[53] R. Yamada,[50] M. Yan,[61] T. Yasuda,[50] Y.A. Yatsunenko,[35] K. Yip,[73] H.D. Yoo,[77] S.W. Youn,[53] C. Yu,[13] J. Yu,[78] A. Yurkewicz,[72] A. Zatserklyaniy,[52] C. Zeitnitz,[25] D. Zhang,[50] T. Zhao,[82] B. Zhou,[64] J. Zhu,[72] M. Zielinski,[71] D. Zieminska,[54] A. Zieminski,[54] V. Zutshi,[52] and E.G. Zverev[37]

(DØ Collaboration)

[1] *Universidad de Buenos Aires, Buenos Aires, Argentina*
[2] *LAFEX, Centro Brasileiro de Pesquisas Físicas, Rio de Janeiro, Brazil*
[3] *Universidade do Estado do Rio de Janeiro, Rio de Janeiro, Brazil*
[4] *Instituto de Física Teórica, Universidade Estadual Paulista, São Paulo, Brazil*
[5] *University of Alberta, Edmonton, Alberta, Canada, Simon Fraser University, Burnaby, British Columbia, Canada, York University, Toronto, Ontario, Canada, and McGill University, Montreal, Quebec, Canada*
[6] *University of Science and Technology of China, Hefei, People's Republic of China*
[7] *Universidad de los Andes, Bogotá, Colombia*
[8] *Center for Particle Physics, Charles University, Prague, Czech Republic*
[9] *Czech Technical University, Prague, Czech Republic*
[10] *Center for Particle Physics, Institute of Physics, Academy of Sciences of the Czech Republic, Prague, Czech Republic*
[11] *Universidad San Francisco de Quito, Quito, Ecuador*
[12] *Laboratoire de Physique Corpusculaire, IN2P3-CNRS, Université Blaise Pascal, Clermont-Ferrand, France*
[13] *Laboratoire de Physique Subatomique et de Cosmologie, IN2P3-CNRS, Universite de Grenoble 1, Grenoble, France*
[14] *CPPM, IN2P3-CNRS, Université de la Méditerranée, Marseille, France*
[15] *IN2P3-CNRS, Laboratoire de l'Accélérateur Linéaire, Orsay, France*
[16] *LPNHE, IN2P3-CNRS, Universités Paris VI and VII, Paris, France*
[17] *DAPNIA/Service de Physique des Particules, CEA, Saclay, France*
[18] *IPHC, IN2P3-CNRS, Université Louis Pasteur, Strasbourg, France, and Université de Haute Alsace, Mulhouse, France*
[19] *Institut de Physique Nucléaire de Lyon, IN2P3-CNRS, Université Claude Bernard, Villeurbanne, France*
[20] *III. Physikalisches Institut A, RWTH Aachen, Aachen, Germany*
[21] *Physikalisches Institut, Universität Bonn, Bonn, Germany*
[22] *Physikalisches Institut, Universität Freiburg, Freiburg, Germany*
[23] *Institut für Physik, Universität Mainz, Mainz, Germany*
[24] *Ludwig-Maximilians-Universität München, München, Germany*
[25] *Fachbereich Physik, University of Wuppertal, Wuppertal, Germany*
[26] *Panjab University, Chandigarh, India*
[27] *Delhi University, Delhi, India*
[28] *Tata Institute of Fundamental Research, Mumbai, India*
[29] *University College Dublin, Dublin, Ireland*
[30] *Korea Detector Laboratory, Korea University, Seoul, Korea*

[31] SungKyunKwan University, Suwon, Korea
[32] CINVESTAV, Mexico City, Mexico
[33] FOM-Institute NIKHEF and University of Amsterdam/NIKHEF, Amsterdam, The Netherlands
[34] Radboud University Nijmegen/NIKHEF, Nijmegen, The Netherlands
[35] Joint Institute for Nuclear Research, Dubna, Russia
[36] Institute for Theoretical and Experimental Physics, Moscow, Russia
[37] Moscow State University, Moscow, Russia
[38] Institute for High Energy Physics, Protvino, Russia
[39] Petersburg Nuclear Physics Institute, St. Petersburg, Russia
[40] Lund University, Lund, Sweden, Royal Institute of Technology and Stockholm University, Stockholm, Sweden, and Uppsala University, Uppsala, Sweden
[41] Physik Institut der Universität Zürich, Zürich, Switzerland
[42] Lancaster University, Lancaster, United Kingdom
[43] Imperial College, London, United Kingdom
[44] University of Manchester, Manchester, United Kingdom
[45] University of Arizona, Tucson, Arizona 85721, USA
[46] Lawrence Berkeley National Laboratory and University of California, Berkeley, California 94720, USA
[47] California State University, Fresno, California 93740, USA
[48] University of California, Riverside, California 92521, USA
[49] Florida State University, Tallahassee, Florida 32306, USA
[50] Fermi National Accelerator Laboratory, Batavia, Illinois 60510, USA
[51] University of Illinois at Chicago, Chicago, Illinois 60607, USA
[52] Northern Illinois University, DeKalb, Illinois 60115, USA
[53] Northwestern University, Evanston, Illinois 60208, USA
[54] Indiana University, Bloomington, Indiana 47405, USA
[55] University of Notre Dame, Notre Dame, Indiana 46556, USA
[56] Purdue University Calumet, Hammond, Indiana 46323, USA
[57] Iowa State University, Ames, Iowa 50011, USA
[58] University of Kansas, Lawrence, Kansas 66045, USA
[59] Kansas State University, Manhattan, Kansas 66506, USA
[60] Louisiana Tech University, Ruston, Louisiana 71272, USA
[61] University of Maryland, College Park, Maryland 20742, USA
[62] Boston University, Boston, Massachusetts 02215, USA
[63] Northeastern University, Boston, Massachusetts 02115, USA
[64] University of Michigan, Ann Arbor, Michigan 48109, USA
[65] Michigan State University, East Lansing, Michigan 48824, USA
[66] University of Mississippi, University, Mississippi 38677, USA
[67] University of Nebraska, Lincoln, Nebraska 68588, USA
[68] Princeton University, Princeton, New Jersey 08544, USA
[69] State University of New York, Buffalo, New York 14260, USA
[70] Columbia University, New York, New York 10027, USA
[71] University of Rochester, Rochester, New York 14627, USA
[72] State University of New York, Stony Brook, New York 11794, USA
[73] Brookhaven National Laboratory, Upton, New York 11973, USA
[74] Langston University, Langston, Oklahoma 73050, USA
[75] University of Oklahoma, Norman, Oklahoma 73019, USA
[76] Oklahoma State University, Stillwater, Oklahoma 74078, USA
[77] Brown University, Providence, Rhode Island 02912, USA
[78] University of Texas, Arlington, Texas 76019, USA
[79] Southern Methodist University, Dallas, Texas 75275, USA
[80] Rice University, Houston, Texas 77005, USA
[81] University of Virginia, Charlottesville, Virginia 22901, USA
[82] University of Washington, Seattle, Washington 98195, USA

(Dated: September 25, 2006)

We present a measurement of the fraction f_+ of right-handed W bosons produced in top quark decays, based on a candidate sample of $t\bar{t}$ events in the ℓ+jets and dilepton decay channels corresponding to an integrated luminosity of 370 pb^{-1} collected by the DØ detector at the Fermilab Tevatron $p\bar{p}$ Collider at $\sqrt{s} = 1.96$ TeV. We reconstruct the decay angle θ^* for each lepton. By comparing the $\cos\theta^*$ distribution from the data with those for the expected background and signal for various values of f_+, we find $f_+ = 0.056 \pm 0.080\,(\text{stat}) \pm 0.057\,(\text{syst})$. ($f_+ < 0.23$ at 95% C.L.), consistent with the standard model prediction of $f_+ = 3.6 \times 10^{-4}$.

PACS numbers: 14.65.Ha, 14.70.Fm, 12.15.Ji, 12.38.Qk, 13.38.Be, 13.88.+e

The top quark is by far the heaviest of the known fermions and is the only one that has a Yukawa coupling of order unity to the Higgs boson in the standard model. We search for evidence of new physics in $t \to Wb$ decay by measuring the helicity of the W boson. In the standard model, the top quark decays via the $V-A$ charged current interaction, almost always to a W boson and a b quark. For any linear combination of V and A currents at the $t \to Wb$ vertex, the fraction f_0 of longitudinally-polarized W bosons is 0.697 ± 0.012 [1] at the world average top quark mass m_t of 172.5 ± 2.3 GeV [2].

In this analysis, we fix f_0 at 0.70 and measure the positive helicity fraction f_+. In the standard model, f_+ is predicted at next-to-leading order to be 3.6×10^{-4} [3]. A measurement of f_+ that differs significantly from this value would be an unambiguous indication of new physics. For example, an f_+ value of 0.30 would indicate a purely $V+A$ charged current interaction.

Measurements of the $b \to s\gamma$ decay rate have indirectly limited the $V+A$ contribution in top quark decays to less than a few percent [4]. Direct measurements of the $V+A$ contribution are still necessary because the limit from $b \to s\gamma$ assumes that the electroweak penguin contribution is dominant. Direct measurements of the longitudinal fraction found $f_0 = 0.91 \pm 0.39$ [5] and $f_0 = 0.56 \pm 0.31$ [6]. Direct measurements of f_+ have set limits of $f_+ < 0.18$ [7], $f_+ < 0.24$ [8], and $f_+ < 0.25$ [9] at the 95% C.L. The analysis presented in this Letter improves upon that reported in Ref. [9] by using a larger data set, including the dilepton decay channel of the $t\bar{t}$ pair, and employing enhanced analysis techniques.

The angular distribution of the down-type decay products of the W boson (charged lepton or d, s quark) in the rest frame of the W boson can be described by introducing the decay angle θ^* of the down-type particle with respect to the top quark direction. The dependence of the distribution of $\cos\theta^*$ on f_+,

$$\omega(c_{\theta^*}) \propto 2(1-c_{\theta^*}^2)f_0 + (1-c_{\theta^*})^2 f_- + (1+c_{\theta^*})^2 f_+ \quad (1)$$

where $c_\theta^* = \cos\theta^*$, forms the basis for our measurement. We proceed by selecting a data sample enriched in $t\bar{t}$ events, reconstructing the four vectors of the two top quarks and their decay products, and then calculating $\cos\theta^*$. This distribution in $\cos\theta^*$ is compared with templates for different f_+ values, suitably corrected for background and reconstruction effects, using a binned maximum likelihood method. In the ℓ+jets channel, the kinematic reconstruction is done with a fit that constrains the W boson mass to its measured value and the top quark mass to 175 GeV, while in the dilepton channel, the kinematics are solved algebraically with the top quark mass fixed to 172.5 GeV.

The DØ detector [10] comprises three main systems: the central tracking system, the calorimeters, and the muon system. The central-tracking system is located within a 2 T solenoidal magnet. The next layer of detection involves three liquid-argon/uranium calorimeters: a central section covering pseudorapidities [11] $|\eta| \lesssim 1$, and two end calorimeters extending coverage to $|\eta| \approx 4$, all housed in separate cryostats. The muon system is located outside the calorimetry, and consists of a layer of tracking detectors and scintillation trigger counters before 1.8 T toroids, followed by two similar layers after the toroids.

This measurement uses a data sample recorded with the DØ experiment and corresponds to an integrated luminosity of about 370 pb^{-1} of $p\bar{p}$ collisions at $\sqrt{s} = 1.96$ TeV. The data sample consists of $t\bar{t}$ candidate events from the ℓ+jets decay channel $t\bar{t} \to W^+W^-b\bar{b} \to \ell\nu qq'b\bar{b}$ and the dilepton channel $t\bar{t} \to W^+W^-b\bar{b} \to \ell\nu\ell'\nu'b\bar{b}$, where ℓ and ℓ' are electrons or muons. The ℓ+jets final state is characterized by one charged lepton, at least four jets (two of which are b jets), and significant missing transverse energy ($\not\!\!E_T$). The dilepton final state is characterized by two charged leptons of opposite sign, at least two jets, and significant $\not\!\!E_T$.

We simulate $t\bar{t}$ signal events with $m_t = 172.5$ GeV for different values of f_+ with the ALPGEN Monte Carlo (MC) program [12] for the parton-level process (leading order) and PYTHIA [13] for gluon radiation and subsequent hadronization. As the interference term between $V-A$ and $V+A$ is suppressed by the small mass of the b quark and is therefore negligible [14], samples with $f_+ = 0.00$ and $f_+ = 0.30$ are used to create $\cos\theta^*$ templates for any f_+ value by a linear interpolation of the templates.

The MC samples used to model background events with real leptons are also generated using ALPGEN and PYTHIA. Backgrounds in the ℓ+jets channel arise predominantly from W+jets production and multijet production where one of the jets is misidentified as a lepton and spurious $\not\!\!E_T$ appears due to mismeasurement of the transverse energy in the event.

The ℓ+jets event selection [15] requires an isolated lepton (e or μ) with transverse momentum $p_T > 20$ GeV, no other lepton with $p_T > 15$ GeV in the event, $\not\!\!E_T > 20$ GeV, and at least four jets. Electrons are required to have $|\eta| < 1.1$ and are identified by their energy deposition and isolation in the calorimeter, their transverse and longitudinal shower shapes, and information from the tracking system. Also, a discriminant combining the above information must be consistent with the expectation for a high-p_T isolated electron [15]. Muons are identified using information from the muon and tracking systems, and must satisfy isolation requirements based on the energies of calorimeter clusters and the momenta of tracks around the muon. They are required to have $|\eta| < 2.0$ and to be isolated from jets. Jets are reconstructed using the Run II mid-point cone algorithm with cone radius 0.5 [16], and are required to have rapidity $|y| < 2.5$ and $p_T > 20$ GeV.

We determine the number of multijet background events N_{mj} from the data, using the technique described in Ref. [15]. We calculate N_{mj} for each bin in the $\cos\theta^*$ distribution from the data sample to obtain the multijet $\cos\theta^*$ templates.

To discriminate between $t\bar{t}$ pair production and background, a discriminant $\mathcal{D}$ with values in the range 0 to 1 is calculated using input variables which exploit differences in kinematics and jet flavor. The kinematic variables considered are: H_T (defined as the scalar sum of the jet p_T values), the minimum dijet mass of the jet pairs $m_{jj\min}$, the χ^2 from the

kinematic fit, the difference in azimuthal angle $\Delta\phi$ between the lepton and $\not\!\!E_T$ directions, and aplanarity $\mathcal{A}$ and sphericity $\mathcal{S}$ [17] (calculated from the four leading jets and the lepton). Only the four leading jets in p_T are considered in computing these variables.

We utilize the fact that background jets arise mostly from light quarks or gluons while two of the jets in $t\bar{t}$ events arise from b quarks by considering the impact parameters with respect to the primary vertex of all tracks within the jet cone. Based on these values, we calculate the probability P_{PV} for each jet to originate from the primary vertex. We then average the two smallest P_{PV} values to form a continuous variable $\langle P_{PV}\rangle$ that tends to be small for $t\bar{t}$ events and large for backgrounds. This approach results in similar background discrimination but better efficiency than applying a simple cut on P_{PV}.

The discriminant is built separately for the e+jets and μ+jets channels, using the method described in Refs. [15, 18]. Background events tend to have $\mathcal{D}$ values near 0, while $t\bar{t}$ events tend to have values near 1. We consider all possible combinations of the above variables for use in the discriminant, and all possible requirements on the $\mathcal{D}$ value, and choose the variables and $\mathcal{D}$ criterion that give the smallest expected uncertainty on f_+. In the e+jets channel, $\mathcal{S}$, H_T, $\langle P_{PV}\rangle$, and χ^2 are used, and $\mathcal{D}$ is required to be > 0.65. In the μ+jets channel, $\mathcal{A}$, H_T, $m_{jj\mathrm{min}}$, $\langle P_{PV}\rangle$, χ^2, and $\Delta\phi$ are used, and $\mathcal{D}$ is required to be > 0.80. In both channels the efficiency for $t\bar{t}$ events to satistfy the $\mathcal{D}$ requirement is independent of the value of f_+.

We then perform a binned Poisson maximum likelihood fit to compare the observed distribution of events in $\mathcal{D}$ to the sum of the distributions expected from $t\bar{t}$, W+jets, and multijet events. N_{mj} is constrained to the expected value within the known uncertainty. The likelihood is then maximized with respect to the numbers of $t\bar{t}$, W+jets, and multijet events, which are multiplied by the appropriate efficiency for the $\mathcal{D}$ selection to determine the composition of the sample used for measuring $\cos\theta^*$.

In the dilepton channel, backgrounds arise from processes such as WW+jets or Z+jets. These processes are either rare or require false $\not\!\!E_T$ from mismeasurement of jet and lepton energy, allowing a good signal to background ratio to be attained using only kinematic selection criteria. The selection is detailed in Ref. [19]. Events are required to have two leptons with opposite charge and $p_T > 15$ GeV and two or more jets with $p_T > 20$ GeV and $|y| < 2.5$. Additional criteria are applied in the ee and $\mu\mu$ channels to suppress $Z \to \ell\ell$, and in the $e\mu$ channel the sum of the two leading jet p_T's and the leading lepton p_T must be greater than 122 GeV. We place a more stringent requirement on electron identification than is used in Ref. [19].

Table I lists the composition of each sample as well as the number of observed events in the data. We observe a disparity between the number of $t\bar{t}$ events in the e+jets channel and μ+jets channel, which is unexpected since the selection efficiencies for the two channels are similar. The statistical significance of the discrepancy in the event distribution is slightly above 2σ. The disparity appears to be a feature of the data sample used in this analysis, as it occurs regardless of the choice of variables used to define $\mathcal{D}$. Further, it has no direct impact on this analysis, which relies only upon the distribution of events in $\cos\theta^*$.

TABLE I: Number of events observed in each $t\bar{t}$ decay channel, the background level as determined by a fit to the $\mathcal{D}$ distribution in the ℓ+jets channels and the expectation from the background production rate and selection efficiency in the dilepton channels, and the expected signal yield assuming standard model $t\bar{t}$ production with a top quark mass of 175 GeV.

	Observed	Background	Expected $t\bar{t}$
e + jets	51	5.3 ± 0.9	32.9
μ + jets	19	3.3 ± 0.4	26.4
$e\mu$	15	2.2 ± 0.6	8.9
ee	4	0.8 ± 0.2	3.3
$\mu\mu$	1	0.4 ± 0.1	2.4

The top quark and W boson four-momenta in the selected ℓ+jets events are reconstructed using a kinematic fit which is subject to these constraints: two jets must form the invariant mass of the W boson, the lepton and the $\not\!\!E_T$ together with the neutrino p_z component must form the invariant mass of the W boson, and the masses of the two reconstructed top quarks must be 175 GeV. Among the twelve possible jet combinations, the solution with the minimal χ^2 from the kinematic fit is chosen; MC studies show this yields the correct solution in about 60% of all cases. The $\cos\theta^*$ distribution obtained in the ℓ+jets data after the full selection and compared to standard and $V + A$ model expectations is shown in Fig. 1(a).

Dilepton events are rarer than ℓ+jets events, but have the advantage that $\cos\theta^*$ can be calculated for each lepton, thus providing two measurements per event. The presence of two neutrinos in the dilepton final state makes the system kinematically underconstrained. However, if a top quark mass is assumed, the kinematics can be solved algebraically with a four-fold ambiguity in addition to the two-fold ambiguity in pairing jets with leptons. For each lepton, we calculate the value of $\cos\theta^*$ resulting from each solution with each of the two leading jets associated with the lepton. To account for detector resolution we repeat the above procedure 100 times, fluctuating the jet and lepton energies within their resolutions for each iteration. The average of these values is taken as the $\cos\theta^*$ for that lepton. The $\cos\theta^*$ distribution obtained in dilepton data is shown in Fig. 1(b).

We compute the binned Poisson likelihood $L(f_+)$ for the data to be consistent with the sum of signal and background templates at each of seven chosen f_+ values. A parabola is fit to the $-\ln[L(f_+)]$ points to determine the likelihood as a function of f_+.

Systematic uncertainties are evaluated in ensemble tests by varying the parameters (see Table II) which can affect the shapes of the $\cos\theta^*$ distributions or the relative contribution from signal and background sources. Ensembles are formed

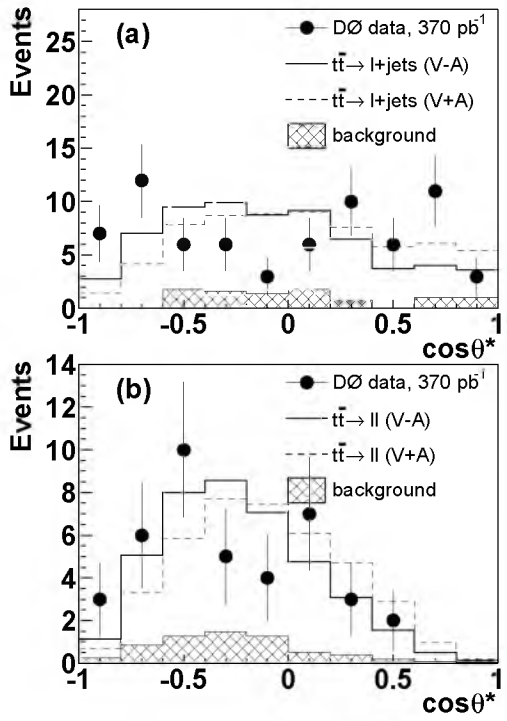

FIG. 1: $\cos\theta^*$ distribution observed in (a) ℓ+jets and (b) dilepton events. The standard model prediction is shown as the solid line, while a model with a pure $V+A$ interaction would result in the distribution given by the dashed line.

by drawing events from a model with the parameter under study varied. These are compared to the standard $\cos\theta^*$ templates in a maximum likelihood fit. The average shift in the resulting f_+ value is taken as the systematic uncertainty and is shown in Table II. The total systematic uncertainty is then taken into account in the likelihood by convoluting the latter with a Gaussian with a width that corresponds to the total systematic uncertainty. The dominant uncertainties arise from the uncertainties on the top quark mass and on the jet energy scale (JES). The mass of the top quark is varied by ± 2.3 GeV and the JES by $\pm 1\sigma$ around their nominal values.

The statistical uncertainty on the $\cos\theta^*$ templates is taken as a systematic uncertainty estimated by fluctuating the templates according to their statistical uncertainty, and noting the RMS of the resulting distribution when fitting to the data.

The effect of gluon radiation in the modeling of $t\bar{t}$ events is studied with an alternate MC sample that includes $t\bar{t}$ events generated with an additional hard parton by ALPGEN. These events are mixed with the standard $t\bar{t}$ events according to the ratio of the leading order cross sections for these two processes. Effects of the chosen factorization scale Q in the generation of the W+jets events are evaluated using a sample generated with a different choice of Q. The systematic uncertainty on the jet flavor composition in the W+jets background is derived using alternate MC samples in which the fraction of b and c jets are varied by 20% about the nominal value [20]. The difference found between the input f_+ value and the reconstructed f_+ value in ensemble tests is taken as the systematic uncertainty on the calibration of the analysis.

TABLE II: Systematic uncertainties on f_+ for the two channels and for their combination.

Source	ℓ+jets	Dilepton	Combined
Jet energy scale	0.038	0.039	0.038
Top quark mass	0.019	0.028	0.021
Template statistics	0.037	0.024	0.028
$t\bar{t}$ model	0.006	0.018	0.009
Background model	0.007	0.007	0.005
Heavy flavor fraction	0.018	–	0.015
Calibration	0.018	0.010	0.016
Total	0.063	0.059	0.057

The systematic uncertainties are conservatively assumed to be fully correlated except for those due to template statistics and the calibration of the individual analyses, which are completely uncorrelated, and the MC model systematic uncertainties which are partially correlated. Assuming a fixed value of 0.7 for f_0, we find

$$f_+ = 0.109 \pm 0.094(\text{stat}) \pm 0.063(\text{syst}) \quad (2)$$

using ℓ+ jets events, and

$$f_+ = -0.089 \pm 0.154(\text{stat}) \pm 0.059(\text{syst}) \quad (3)$$

using dilepton events. Combination of these results yields

$$f_+ = 0.056 \pm 0.080(\text{stat}) \pm 0.057(\text{syst}). \quad (4)$$

We also calculate a Bayesian confidence interval (using a flat prior distribution which is non-zero only in the physically allowed region of $f_+ = 0.0 - 0.3$) which yields

$$f_+ < 0.23 \ @\ 95\%\ \text{C.L.} \quad (5)$$

As seen in Fig. 1(a), there is a deficit of ℓ+jets data events in the central region of $\cos\theta^*$. We estimate the significance of this effect by performing a likelihood ratio test to evaluate the goodness-of-fit for the best-fit model and find that the probability of obtaining a worse fit is 1.3%. We also evaluate the goodness of fit for the standard model hypothesis and find a fit probability of 0.8% (statistical). Thus we conclude that the discrepancy is not statistically significant. We have studied the subset of our MC ensemble tests in which the mock data has a lower fit probability than the collider data does and find that our sensitivity to the value of f_+ in this subset is the same as in the entire set of ensembles.

In summary, we have measured the fraction of right-handed W bosons in $t\bar{t}$ decays in the ℓ+jets and dilepton channels, and find $f_+ = 0.056 \pm 0.080(\text{stat}) \pm 0.057(\text{syst})$. This is the most precise measurement of f_+ to date and is consistent with the standard model prediction of $f_+ = 3.6 \times 10^{-4}$ [3].

We thank the staffs at Fermilab and collaborating institutions, and acknowledge support from the DOE and NSF (USA); CEA and CNRS/IN2P3 (France); FASI, Rosatom and RFBR (Russia); CAPES, CNPq, FAPERJ, FAPESP and

FUNDUNESP (Brazil); DAE and DST (India); Colciencias (Colombia); CONACyT (Mexico); KRF and KOSEF (Korea); CONICET and UBACyT (Argentina); FOM (The Netherlands); PPARC (United Kingdom); MSMT (Czech Republic); CRC Program, CFI, NSERC and WestGrid Project (Canada); BMBF and DFG (Germany); SFI (Ireland); The Swedish Research Council (Sweden); Research Corporation; Alexander von Humboldt Foundation; and the Marie Curie Program.

[*] On leave from IEP SAS Kosice, Slovakia.
[†] Visitor from Helsinki Institute of Physics, Helsinki, Finland.
[‡] Visitor from Lewis University, Romeoville, IL, USA

[1] G. L. Kane, G. A. Ladinsky, and C.-P. Yuan, Phys. Rev. D **45**, 124 (1992); R. H. Dalitz and G. R. Goldstein, *ibid.*, 1531; C. A. Nelson *et al.*, Phys. Rev. D **56**, 5928 (1997).
[2] TeVatron Electroweak Working Group, hep-ex/0603039.
[3] M. Fischer *et al.*, Phys. Rev. D **63**, 031501(R) (2001).
[4] K. Fujikawa and A. Yamada, Phys. Rev. D **49**, 5890 (1994); P. Cho and M. Misiak, Phys. Rev. D **49**, 5894 (1994); C. Jessop, SLAC-PUB-9610.
[5] CDF Collaboration, T. Affolder *et al.*, Phys. Rev. Lett. **84**, 216 (2000).
[6] DØ Collaboration, V. M. Abazov *et al.*, Phys. Lett. B **617**, 1 (2005).
[7] CDF Collaboration, D. Acosta *et al.*, Phys. Rev. D **71**, 031101 (2005).
[8] CDF Collaboration, A. Abulencia *et al.*, Phys. Rev. D **73**, 111103 (2006).
[9] DØ Collaboration, V. M. Abazov *et al.*, Phys. Rev. D **72**, 011104(R) (2005).
[10] DØ Collaboration, V. M. Abazov *et al.*, Nucl. Instrum. Methods A **565**, 463 (2006).
[11] Rapidity y and pseudorapidity η are defined as functions of the polar angle θ with respect to the proton beam and the parameter β as $y(\theta,\beta) \equiv \frac{1}{2}\ln[(1+\beta\cos\theta)/(1-\beta\cos\theta)]$ and $\eta(\theta) \equiv y(\theta,1)$, where β is the ratio of a particle's momentum to its energy.
[12] M. L. Mangano *et al.*, JHEP **07**, 001 (2003).
[13] T. Sjöstrand *et al.*, Comp. Phys. Commun. **135**, 238 (2001).
[14] C.A. Nelson *et al.*, Phys. Rev. D **56**, 5928 (1997).
[15] DØ Collaboration, V. M. Abazov *et al.*, Phys. Lett. B **626**, 45 (2005).
[16] G.C. Blazey *et al.*, hep-ex/0005012.
[17] V. Barger *et al.*, Phys. Rev. D **48**, 3953 (1993).
[18] DØ Collaboration, B. Abbott *et al.*, Phys. Rev. D **58**, 052001 (1998).
[19] DØ Collaboration, V. M. Abazov *et al.*, "Measurement of the $t\bar{t}$ Production Cross Section in $p\bar{p}$ Collisions Using Dilepton Events", in preparation.
[20] DØ Collaboration, V. M. Abazov *et al.*, Phys. Lett. B **626**, 35 (2005)